Romanian Reports in Physics, Vol. 60, No. 3, P. 735–748, 2008

Dedicated to Prof. Ioan-Iovitz Popescu's 75th Anniversary

DEFECTS IN SILICON: FROM BULK CRYSTALS TO NANOSTRUCTURES

M. L. CIUREA[1], V. IANCU[2], S. LAZANU[1], A.-M. LEPADATU[1], E. RUSNAC[1], I. STAVARACHE[1]

[1] *National Institute of Materials Physics, 105 bis Atomistilor Street, P.O. Box MG-7, Bucharest-Magurele 077125, Romania, E-mail: ciurea@infim.ro*
[2] *University "Politehnica" of Bucharest, 313 Splaiul Independentei, Sector 6, Bucharest 060042, Romania, E-mail: codas@physics.pub.ro*

(Received March 26, 2008)

Abstract. Defects in silicon are studied as function of the dimensionality of the investigated structures. Defects produced by strong irradiation in bulk crystals, like vacancies or interstitial defects, induce other defects, so that the irradiated devices are irreversibly damaged. Defects in nanostructures are shown to be produced mainly by surface/interface states and strains, and are therefore specific to the investigated structure. The modeling of the experimental methods allows the determination of defect parameters that are not directly measurable. The carriers capture on quantum confinement levels in 0D systems has a similar behavior with the trapping phenomena.

Key words: Defects, silicon, bulk crystals, nanostructures.

1. INTRODUCTION

There are several phenomena such as the electrical transport and phototransport, the light absorption and emission etc., for which the investigation of defects is essential. Sometimes the defects are useful and sometimes they have to be avoided because they make troubles. In bulk semiconductors, there are specific applications like the radiation detectors where the defects are very useful [1, 2].

Silicon is used in radiation detectors and electronic devices. Nowadays, these devices achieve submicron technology and they are parts of integrated circuits with large to very large scale integration. Silicon and silicon-based devices are commonly operated in many fields of physics including particle physics experiments, nuclear medicine, reactors and space. Defects in the material represent a limiting factor in the operation of devices.

In spite of the effort paid up to now by the scientific community, there are a lot of aspects not clarified, related to the behavior of impurities, and a global understanding of their local structure and properties became increasingly important

due to the reduction in chip sizes and to the increase of the operation speed. The study of effects of point defects on electronic, structural and vibration properties of bulk semiconductors, and also on low size semiconductor structures is a thematic of high interest. This study will bring contributions to the fabrication of Si based smart materials for photonics, MOS and nanowires- based devices etc. The fabrication of new materials can enable revolutionary advances in science and technology.

In bulk semiconductors the trap defects (point defects, impurities and local stresses) are located in the volume of the material. In nanocrystalline semiconductors the trapping phenomena are dominated by the traps located at the surface/interface, due to the very big area/volume ratio (of the order of 10^8 m^{-1} for nanocrystals). These traps are produced by the adsorption, dangling bonds, and the internal stresses (induced by misfit) [3, 4].

There are some methods that can be used to investigate trapping phenomena in both bulk crystals and nanostructures. On the other hand, there are methods that are specific for some kinds of systems and structures. The most used general methods are: the photo-induced current transient spectroscopy (PICTS), the thermally stimulated currents (TSC), the thermally stimulated depolarization currents (TSDC), and the optical charging spectroscopy (OCS).

The aim of this paper is to present some defects specific to crystalline silicon, as function of the dimensionality of the crystals. In Section 2 the defects in bulk silicon are discussed, while in Section 3 the low dimensional systems (2D, 1D and 0D) are analyzed. Section 4 compares the previous results and Section 5 presents the conclusions.

2. DEFECTS IN BULK CRYSTALS

Irradiation is one of the methods used for the introduction of defects into materials, and this is a rather rapid and efficient method, but poorly controllable. The mechanisms of defect production and evolution during and after irradiation are not fully understood, in spite of the research effort of the last half century. The partnership between research and technological development was a real basis for this type of studies. The research in this thematic has been sustained by the large scale utilization of Si as a material for detectors used in terrestrial experiments or in space in physics at high energies.

2.1. INTRINSIC DEFECTS

The stability of crystalline silicon comes from the fact that each silicon atom can accommodate its four valence electrons in four covalent bonds with its four

neighbors. The production of primary defects or the existence of impurities or defects destroys the fourfold coordination.

It has been established that the structural characteristics of the "classical" ***vacancy*** are: the bond length in the bulk is 2.35 Å and the bond angle –109°. The formation energy is 3.01 eV (p-type silicon), 3.17 eV (intrinsic), 3.14 eV (n-type).

For ***interstitials***, different structural configurations are possible: a) the hexagonal configuration, a sixfold coordinated defect with bonds of length 2.36 Å, joining it to six neighbors which are fivefold coordinated; b) the tetrahedral interstitial is fourfold coordinated; has bonds of length 2.44 Å joining it to its four neighbors, which are therefore fivefold coordinated; c) the split – <110> configuration: two atoms forming the defect are fourfold coordinated, and two of the surrounding atoms are fivefold coordinated; d) the 'caged' interstitial contains two normal bonds, of length of 2.32 Å, five longer bonds in the range 2.55÷2.82 Å and three unbounded neighbors at 3.10÷3.35 Å. The calculations [5–7] found that the tetrahedral interstitial and caged interstitial are metastable. For interstitials, the lowest formation energies in eV are 2.80 (for p-type material), 2.98 (for n-type) and 3.31 in the intrinsic case respectively.

It has been established that in silicon the vacancy takes on five different charge states in the band gap: V^{2+}, V^{+}, V^{0}, V^{-}, and V^{2-} and the self-interstitial could exists in four charge states after some authors [8]: I^{-}, I^{0}, I^{+} and I^{2+}, or in five states, after other authors [9, 10].

The experimental examination of primary point defects buried in the bulk is difficult and for various defects this is usually indirect. In a series of theoretical studies [11] and correlated EPR and DLTS experiments of Watkins and co-workers [12], it became possible to solve some problems associated with the electrical level structure of the vacancy. The charge states V^{2+}, V^{+}, V^{0} form the so-called negative U system, caused when the energy gain of a Jahn-Teller distortion is larger than the repulsive energy of the electrons, case in which the (0/+) level is inverted in respect to (+/++) level, which are the striking consequence of the fact that the V^{+} charge state is metastable. The annealing is the result of long range migration of the vacancy. Vacancy is instable and interacts with other defects. Vacancies which have escaped recombination with interstitials become mobile around 100 K. The exact temperature and the activation energy associated with this mobility depend on the charge state.

The interstitial is considered to be mobile at all temperatures in silicon. A possible explanation of its athermal migration is the Bourgoin mechanism [13]: it is assumed that the defect can exist in more than one charge state and there is sequential trapping and detrapping of charge carriers generated by the ionization which occurs throughout the period of electron irradiation. There is no direct proof of the isolated interstitials existence in silicon, and their presence has been deduced from both theory and displacement from substitutional to interstitial impurities positions.

Up to now, nothing is experimentally known about self interstitial annealing processes. In the old Dienes and Damask's papers [14], the authors proposed the formation of diinterstitial, but this defect was not experimentally evidenced. Interstitials are associated with possible mechanisms of complex defects formation. Recently, Lindstroem and co-workers [15] reported in IR studies, the experimental identification of possible annealing reactions, initiated by silicon self interstitials (see equations from 8 to 14, 15 and 17 in their up-cited paper). Only recently, Lukjanitsa [8] identified experimentally all the energy levels assigned to vacancies and interstitials. In Tables 1 and 2, we present a review of the present knowledge on energy levels in the band gap for isolated vacancies and interstitials, as experimental data and model calculation together with the corresponding charge states.

Table 1

Energy levels of isolated vacancies in silicon

Vacancy			
Energy level [eV]		Reference	Assigned charge state
Experimental	Calculated		
$E_v + 0.05$		[12]	$V^{+/0}$
$E_v + 0.13$		[12]	$V^{2+/+}$
	$E_v + 0.36$	[16]	$V^{0/-}$
$E_v + 0.47$		[8]	Non attributed
	$E_v + 0.76$	[17]	Non attributed
$E_v + 0.84$	$E_v + 0.84$	[8, 16]	$V^{2-/-}$
$E_v + 1.01$		[18]	$V^{2-/-}$

Table 2

Energy levels of isolated interstitials in silicon

Interstitial			
Energy level [eV]		Reference	Assigned charge state
Experimental	Calculated		
	Ev + 0.12	[17]	Non attributed
$E_v + 0.26$		[8]	Non attributed
	$E_v + 0.4$	[10]	$I^{2+/+}$
$E_v + 0.45$		[8]	Non attributed
	Ev + 0.52	[17]	Non attributed
$E_v + 0.68$	$E_v + 0.7$	[8, 10]	$I^{+/0}$ T-X cross
	Ev + 0.76	[9]	$I^{2+/+}$
	$E_v + 0.9$	[10]	$I^{+/0}$ T-T cross
	Ev + 1.04	[9]	$I^{-/2-}$

In crystalline silicon bombarded with energetic projectiles, ***the divacancy*** center is being studied for about 40 years by numerous authors applying various experimental techniques, *e.g.* EPR [19], photoconductivity [20], infrared absorption [21], electron-nuclear double resonance (ENDOR) or deep level transient spectroscopy (DLTS) and at the room temperature it is considered as a stable defect. The unperturbed configuration of divacancy could be viewed as two vacant, nearest neighbor, lattice sites. The formation mechanism is the reciprocal trapping of two migrating vacancies. Isochronal and isothermal annealing studies have concluded that the divacancy anneals out at 570 K [19]. The mechanisms of V_2 annealing are not fully understood. It is generally agreed now that annealing of V_2 occurs by dissociation and/or annihilation by an impurity or defect with a concentration at least one order of magnitude higher than the V_2. It has been found that annealing of the divacancy-related levels, the singly negative V_2 (0/–), and the doubly negative V_2 (–/=) charge states at 220–300°C results in the formation of a new centre, unknown (noted X) with singly negative, X(0/–), and doubly negative, X(–/=), charge states. The new centre anneals out at 325–350°C during isochronal treatment for 15 min. Some authors [15, 22], based on IR absorption and DLTS measurements, found that its reaction with interstitial oxygen is a possible mechanism for divacancy annealing out and found a possible dependence of its kinetics on impurity concentrations. Pellegrino and co-workers [23], based on DLTS measurements in electron irradiated and Si implanted Si, found that O_i couldn't be the main trap for divacancies, and that the reaction between a divacancy and an interstitial could be of interest only at very high irradiation fluences. The same reaction has been proposed by Davies [24], who couldn't put in evidence such a mechanism by IR absorption.

In 2002, in a highlight contribution, S. Goedecker, T. Deutsch and L. Billard [25] predicted the existence of a ***new type of primary defect*** in silicon and thus a new type of symmetry of the material. It has a ***fourfolded coordinated configuration*** and is more stable. Lazanu and Lazanu, [26], using experimental information from irradiation, established the characteristics of the new defect: energy level is in the middle of the band gap between E_c – (0.46÷0.48) eV, a capture cross section between $(5\div10)\times10^{-15}$ cm^2 and a ratio $\sigma_p/\sigma_n = 1\div5$. The existence of this new type of structure was confirmed by in-situ HRTEM analysis for Si; see Fedina and co-workers [27] and was predicted also for germanium [28].

Interstitials, vacancies, and FFCD defects could aggregate, giving rise to smaller of greater ***clusters***. They are a clue in the understanding of the radiation damage in silicon [29]. Hypotheses on their existence are as old as the study of defects in semiconductors [30], but neither the mechanisms of formation nor clear experimental evidence exist up to now. The subject is of great interest, and different models are proposed [31]. The structural and dynamical properties of Si-interstitial

defects are fundamental for the understanding of dopant dynamics. Small interstitial clusters can provide the growth nuclei for extended defects and can release mobile interstitials leading to enhanced diffusion of dopants at low temperature [32]. Calculations [33] established that compact *interstitial clusters* are favorable for $n = 2–4$, while elongated clusters are energetically favorable for larger clusters. The existence of *vacancy clusters* has been predicted as well. By means of simulations, the formation and binding of vacancy clusters V_n in silicon has been investigated [34]: it was shown that different growth patterns exist and that interplay between energy and topology arguments determines the most stable aggregates.

2.2. COMPLEXES WITH IMPURITIES

The ***VP centre*** is another defect that has been carefully investigated from the remote past: by EPR [35], by IR absorption [36], Hall-effect and electrical-conductivity measurements [37]. It is important in n-type silicon with low oxygen content, being a vacancy trap. It anneals out at around 400 K [38].

In the class of ***V_iO_j complexes***, defects with $i, j = 1, 2, 3, \ldots$ are considered. From these centers, the VO is the best known. V_iO_j complexes generally follow the V_2 and/or VO annealing at higher temperature [39]. The VO centre (A centre) is the main radiation defect induced in oxygen rich samples. It is one of the first and most thoughtfully studied defects in silicon and is formed when interstitial oxygen captures a vacancy. This centre has been put in evidence by EPR [35], IR absorption [36], by Hall-effect and electrical-conductivity measurements [37], by DLTS. The VO centre anneals out at around 620 K [40]. Migration of VO and reaction with O_j, with the formation of VO_2 pairs could be one of the annealing out mechanisms of V_2 (Londos [41] identified the VO_2 centre after irradiation followed by annealing at temperatures higher than 570 K, while Lindstroem [15] identified VO_2 in samples irradiated in the temperature range 300–600 K). The VO_2 centre anneals out at around 720 K, by forming the VO_3. VO_2 and VO_3 are the dominant defects identified by IR absorption after electron irradiation at temperatures in the range 600–800 K. In carbon-lean silicon, another defect, the oxygen dimmer, has been identified. A proposed formation mechanism is the interaction of VO_2 with an interstitial [15], for which the reverse reaction is also possible. In contrast with this situation, in carbon rich samples the oxygen dimmer has not been identified. Other oxygen – vacancy complexes, as V_2O_2 have been identified in the same temperature range, by the same group.

Complexes formed with carbon: The Watkins replacement mechanism [42] is the main mechanism responsible for interstitial disappearance after irradiation, especially in n-type silicon. C_i has been identified by EPR and DLTS [43]. Interstitial carbon anneals in at 160–180 K, and anneals out at 260–280 K. C_i reacts

with impurities (oxygen, carbon, phosphorous) to form stable defects [44]. So, C_i, mobile at room temperature, is captured by a substitutional carbon to form the C_iC_s complex, which anneals out most probably by dissociation [45]. The disappearance of C_iC_s centers during further irradiation has been found, and has been attributed to mechanisms of the type: $C_iC_s + I \rightarrow CCI$ and $CCI + I \rightarrow CCII$ [24], but not experimental evidence exists. C_i could be also be captured by an interstitial oxygen, and form the C_iO_i complex: $C_i + O_i \rightarrow C_iO_i$, identified after irradiation at 300–600 K by IR and DLTS [15, 24]; C_iO_i could capture another interstitial, to form the IC_iO_i centre [24]. To explain the observation that C_iO_i centers disappear at further irradiation, the most probable hypothesis is by the capture of newly formed primary defects. For carbon rich samples, in the irradiation temperature range 600–800 K, the interstitial carbon interacts with vacancy – oxygen centre and forms complexes: $VO_2 + C_i \rightarrow C_iVO_2$ or C_sO_{2i}, and $VO_3 + C_i \rightarrow C_iVO_3$ or C_sO_{3i} [15]. The last two defects are not present in samples irradiated at RT and subsequently annealed.

3. DEFECTS IN NANOSTRUCTURES

3.1. DEFECTS IN 2D STRUCTURES

We will first present some investigations made on multi-quantum well (MQW) structures formed by a set of 50 bilayers of nc-Si and CaF_2 deposited on silicon substrate, $(nc\text{-}Si/CaF_2)_{50}$, by OCS [46, 47] and TSDC [48]. The MQW films were deposited by molecular beam epitaxy on n-type (111) silicon substrate [48, 49]. The thicknesses of the silicon and calcium fluoride layers for the OCS measurements were equal (1.6 nm), while for TSDC measurements the CaF_2 layers had double thickness compared to the Si ones (3 and 1.5 nm respectively).

The OCS method has two steps. First, the sample is cooled down at a low temperature T_0, where it is illuminated. The light wavelength λ is chosen in the absorption band. The photogenerated carriers diffuse with different velocities ($v_n \neq v_p$) into the film and some of them are trapped. These trapped carriers generate a frozen-in electric field. The heating is made after the switch-off of the light and the sample is short-circuited by an electrometer. During the heating, the trapped carriers are released and move under the field of the still trapped ones. Thus, the discharge current depends only on the frozen-in electric field.

Fig. 1 presents the OCS discharge curves measured on MQW [46]. To begin with, a cycle of cooling-heating without illumination was made to find out the sample polarization. The corresponding discharge curve is called “zero curve” (see

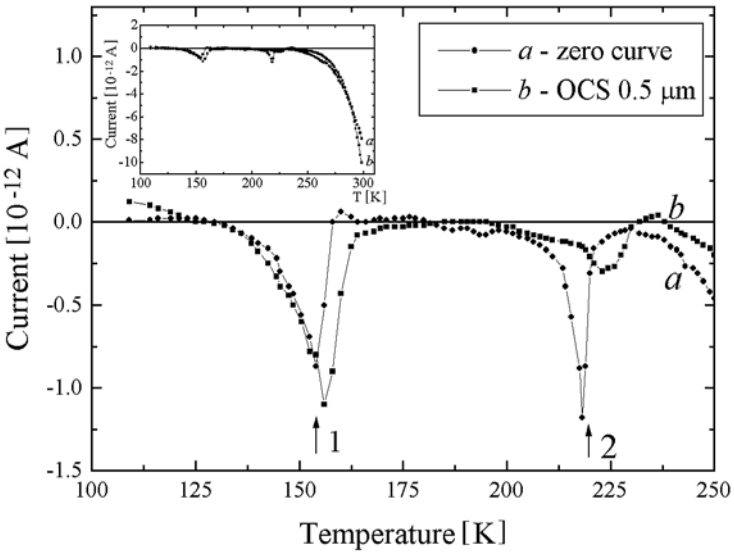

Fig. 1 – OCS discharge current in MQW structure: *a*) zero curve; *b*) OCS curve (λ = 0.5 μm) [46].

Fig.1, curve *a*). Unexpectedly, two spikes located at 152 K and 215 K were observed. The discharge curve after the illumination is shown in Fig. 1, curve *b*. One can see that the first spike from the zero curve also appears in the OCS curve (at 155 K). The second spike is much diminished and shifted to 225 K. At the same time, a supplementary shoulder appears at 230 K. Both curves present a discharge tail towards room temperature (RT). The appearance of the spikes in the zero curve can be understood if we consider the misfit strains induced by the cooling at nc-Si/CaF_2 interfaces. Usually the strains act as traps [50, 51]. The filling of the cooling-induced strain traps depends on the cooling rate.

A fractional heating procedure was used to resolve the second maximum and the neighbor shoulder and then to determine their activation energies. The activation energies evidenced by this procedure are E_1 = 0.30 eV, E_2 = 0.42 eV, E_3 = 0.44 eV, and E_4 = 0.75 eV (the last one corresponds to the final tail).

The same structures were investigated by TSDC. The method has a lower resolution and the position of the only well observed peak is shifted to lower temperatures. The observed activation energy is 0.7–0.8 eV, corresponding to the OCS tail.

Besides MQWs and superlattices, another typical example of a 2D structure is the channel of a CMOS transistor. The traps in the gate dielectric determine a charge accumulation, proportional with the relative dielectric constant κ [52]. As a result, the threshold voltage V_T increases with the ratio between the trapped charge and its capacitance with respect to the substrate ($\Delta V_T = q_t/C_t$). If one attempts to

measure the carrier mobility by using $I_d - V_g$ pulse measurements, the obtained apparent value will then be smaller than the real one, $\mu_a = \mu(1 - \partial\Delta V_T/\partial V_g)$. For high κ dielectric transistors, the decrease can be up to 27%. However, in high frequency transistors, this effect appears only for fast trapping processes. It is to be remarked that, if one uses spin valve structures (*i.e.* strong magnetic orientation), the exclusion principle forbids the charge trapping if the trap and the carrier have parallel spins – see Ref. [53], so that, in this case, the apparent mobility equals the real one even at low frequencies.

3.2. DEFECTS IN 1D STRUCTURES

As a typical example of 1D nanostructure, we have investigated nanocrystalline porous silicon (nc-PS) by OCS [54–56] and TSDC [57]. The nc-PS films were electrochemically etched and then were photochemically processed [57]. The films were stabilized by controlled oxidation. These films present a double scale of porosity [58], a microporosity that consists of a system of alveolar columnar pores, separated by nanoporous walls formed by a nanowire network.

The results of the OCS measurements are presented in Fig. 2 [58]. The observed activation energies are $E_1 = 0.29$ eV; $E_{2'} = 0.37$ eV; $E_{2''} = 0.41$ eV; $E_3 = 0.47$ eV, $E_4 = 0.61$ eV, and $E_5 = 0.82$ eV. The maximum quoted F is a false maximum, with no correlation to any trapping level [56]. One can see that the first four maxima, corresponding to surface traps, are very flattened by the trap healing produced by oxidation. This effect is much stronger for the anodical oxidation (curve *b*) than for the native oxidation (curve *a*, taken for comparison).

The TSDC measurements allowed to evidence only one maximum, with the energy 0.41–0.48 eV (the maxima 2′ and 2″ cannot be resolved by this method).

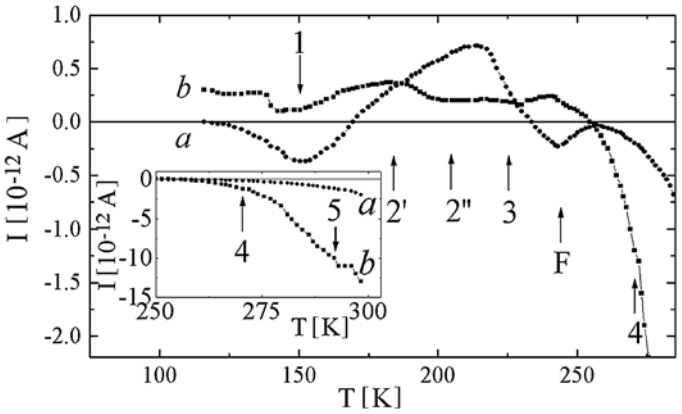

Fig. 2 – OCS discharge current in nc-PS ($\lambda = 0.5$ μm): *a*) natively and *b*) anodicaly oxidized samples [58].

3.3. DEFECTS IN 0D STRUCTURES

The 0D structures introduce two specific aspects in the study of the defects. The first one is that some carriers can be captured on the quantum confinement (QC) levels from a dot. This phenomenon appears as analogous with the real trapping. However, it is not related to any kind of defect, so it introduces false information concerning the trap parameters. The second one is related to the Coulomb blockade. In a dot, the Coulomb repulsion does not allow more than one non-compensated charge. Therefore both trapping and detrapping processes are modified and the information obtained can be strongly affected.

An example of an application using the capture of the carriers on QC levels is a floating gate of memory device consisting of a MOS structure [59]. A very thin (2 nm) SiO_2 layer is deposited on a (100) p-type Si wafer. On this tunneling layer there are fabricated Si dots (7 nm diameter), regularly spaced. These dots are then coated with silicon nitride (1 nm thickness), and all is covered with a 41 nm SiO_2 film and then with a metallic gate. At a negative polarization of the gate, holes are injected from the substrate through the tunneling oxide into the dots. These holes are first captured on the QC levels of the dots and then trapped on the Si/SiN_x interface defects. When changing the polarity, the holes from the QC levels are easily released, while those from the traps remain, ensuring the memory effect.

Another example is a field effect LED with an array of Si dots in the silicon oxide and a semitransparent gate electrode [60]. In A.C. regime, electrons and holes are alternately injected in the dots and form excitons. The excitons recombination will generate photon emission. The important thing is that the current frequency must not be higher than the inverse of the exciton lifetime, otherwise the excitons will not recombine and the light signal will abruptly decrease.

4. DISCUSSION

In bulk crystals, the activation energies for different kinds of defects are computed as the difference between the energy of a structure with a defect (*e.g.* vacancy or interstitial defect) and an ideal structure [10]. The most used way to perform these calculations is the tight binding method [17]. From the Tables 1 and 2, one can see that the calculated values are generally different from the experimental ones. This can be due to improper modeling or to improper attribution of the experimental values to specific defects.

Concerning the nanostructures, the information directly resulting from the OCS measurements is rather poor regarding the determining of the trap parameters. Therefore we have modeled the trapping-detrapping-retrapping processes during the OCS measurements and the corresponding discharge current as function of the

temperature [47, 56]. This way, using the activation energies as input data, we have corrected their values and also determined the trap concentrations, the capture cross-sections and the carrier lifetimes, as well as information about the trapping centers localization (in the bulk or at the surface/interface) and about the sign of the trapped carriers.

The results obtained from the modeling of the OCS measurements on MQW structures are presented in Table 3 [47]. The centre type is n or p (for the sign of the trapped carriers) and S or B (for surface or bulk localization). Table 4 presents similar results obtained on fresh nc-PS [56]. The fresh sample was preferred because the surface traps are not healed and the corresponding maxima are more pronounced.

Table 3

Values of the parameters for MQW trapping centers

Maximum number	Centre type	σ [10^{-18} cm^2]	N_t (P_t) [10^{15} cm^{-3}]	τ [μs]	E_t [eV]
1	n S	1.70	6.600	0.40	0.30
2	n S	0.41	2.600	0.40	0.42
3	p S	1.00	0.029	0.18	0.44
4	n S	1.50	5.500	0.40	0.72

Table 4

Values of the parameters for nc-PS trapping centers

Maximum number	Centre type	σ [10^{-18} cm^2]	N_t (P_t) [10^{12} cm^{-3}]	τ [μs]	E_t [eV]
1	p S	3.00	1.800	0.05	0.30
2′	p S	3.00	1.500	0.05	0.37
2″	n S	1.50	0.250	0.05	0.41
3	n S	0.90	1.400	0.05	0.47
4	p B	3.00	0.085	0.15	0.61

When one attempts to compare the different activation energies, one can see that they are different. The agreements between $E_2 = 0.42$ eV (MQW) and $E_{2''} = 0.41$ eV (nc-PS), and between $E_{exp4} = 0.84$ eV (bulk vacancy) and $E_5 = 0.82$ eV (nc-PS), respectively, are only apparent. Indeed, the bulk defects analyzed in this paper (vacancies and interstitial defects) are induced by aggressive methods (strong irradiation), while the defects in nanocrystals are mainly related to surface/interface states and to strains. Thus, the trapping levels 1, 2, and 4 from MQW samples are due to the misfit strains produced by the cooling/heating cycles, while level 3 is probably a specific Si/CaF_2 interface trap. On the other hand, the surface traps observed in fresh nc-PS samples are related to surface states, as they are healed by oxidation. On the contrary, the bulk traps in stabilized nc-PS are due to the strains induced by oxidation. At the same time, the carrier capture on QC levels in 0D systems has no equivalent in 1D, 2D or 3D structures.

5. CONCLUSIONS

Defects in silicon, both bulk crystals and nanostructures, were experimentally investigated by means of different methods, some general and some specific. The results were modeled to obtain maximum possible information from the experimental data.

In the case of bulk silicon, our aim was to analyze the defects produced with high concentration by strong irradiation. The most damaging ones are those with the energy levels in the band gap, which are sources for non-radiative generation – recombination and trapping processes. They induce irreversible changes in the operational parameters of the devices submitted to irradiation.

In the case of nanostructures, the defects are generally induced by surface/ interface states and strains and are therefore specific to the investigated structure. This is why there is no correspondence between the activation energies measured in bulk crystals and in different nanostructures. On the other hand, by an appropriate modeling, one can find the values of several trap parameters (*e.g.* trap concentrations, capture cross-sections, detrapped carrier lifetimes etc.) that are not directly measurable. The 0D systems present supplementary carriers capture on QC levels, as well as specific behavior induced by the Coulomb blockade.

The traps in nanostructures, as well as those in bulk crystals, have a strong influence on the working regimes and the reliability of the devices based on such structures. This is the reason why the material research studies are more and more focused on "defect engineering".

Acknowledgements. Financial support from the Romanian National University Research Council grant No. 849/2007 and from Research for Excellency Program CEEX contract No. Cx-0611-13 is acknowledged.

REFERENCES

1. R. Siemieniec, W. Südkamp, J. Lutz, Sol. St. Electron., **46**, 891–901 (2002).
2. G. Kramberger, V. Cindro, I. Mandić, M. Mikuž, M. Zavrtanik, Nucl. Instr. Meth. Phys. Res. A, **516**, 109–115 (2004).
3. D. A. Faux, J. R. Downes, E. P. O'Reilly, J. Appl. Phys., **82**, 3754–3762 (1997).
4. A. Benfilda, Proc. 1st Int. Workshop Semicond. Nanocryst. SEMINANO 2005, Budapest 2005; **1**, 123–126.
5. R. J. Needs, J. Phys. Condens. Matter **11**, 10437–10450 (1999).
6. W.-K. Leung, R. J. Needs, G. Rajagopal, S. Itoh, S. Ihara, Phys. Rev. Lett., **83**, 2351–2354 (1999).
7. S. J. Clark, G. J. Ackland, Phys. Rev. B, **56**, 47–50 (1997).
8. V. V. Lukianitsa, Semiconductors, **37**, 404–413 (2003).
9. J. L. Mozos, R. M. Nieminen, *Properties of crystalline silicon,* ed. R. Hull, EMIS, London, 1998.
10. G. M. Lopez, V. Fiorentini, Phys. Rev. B, **69**, 155206–155213 (2004).

11. G. A. Baraff, E. O. Kane, M. Schlüter, Phys. Rev. Lett., **43**, 956–959 (1979).
12. G. D. Watkins, J. R. Troxell, Phys. Rev. Lett., **44**, 593–596 (1980).
13. J. C. Bourgoin, J. W. Corbett, Rad. Effects, **36**, 157–188 (1978).
14. G. J Dienes, A. C. Damask, Phys. Rev., **128**, 2542–2546 (1962); Phys. Rev., **125**, 447–450 (1962).
15. J. L. Lindstroem, L. I. Murin, T. Hallberg, V. P. Markevich, B. G. Svensson, M. Kleverman, J. Hermansson, Nucl. Instr. Meth. Phys. Res. B, **186**, 121–125 (2002).
16. J. A. Van Vechten, Phys. Rev. B, **33**, 2674–2689 (1986).
17. E. G. Song, E. Kim, Y. H. Lee, Y. G. Hwang, Phys. Rev. B, **48**, 1486–1489 (1993).
18. P. M. Fahey, P. B. Griffin, J. D. Plummer, Rev. Mod. Phys., **61**, 289–384 (1989).
19. G. D. Watkins, J. W. Corbett, Phys. Rev., **138**, A543–A555 (1965).
20. A. H. Kalma, J. C. Corelli, Phys. Rev., **173**, 734–745 (1968).
21. L. J. Cheng, J. C. Corelli, J. W. Corbett, G. D. Watkins, Phys. Rev., **152**, 761–774 (1966).
22. E. V. Monakhov, B. S. Avset, A. Hallén, B. G. Svensson, Phys. Rev. B, **65**, 233207 (2002).
23. P. Pellegrino, P. Lévêque, J. Lalita, A. Hallén, C. Jagadish, B. G. Svensson, Phys. Rev. B, **64**, 195211 (2001).
24. G. Davies, E. C. Lightowlers, R. C. Newman, A. S. Oates, Semicond. Sci. Technol., **2**, 524–532 (1987).
25. S. Goedecker, T. Deutsch, L. Billard, Phys. Rev. Lett., **88**, 235501–235504 (2002).
26. I. Lazanu, S. Lazanu, Phys. Scr., **74**, 201–207 (2006).
27. L. I. Fedina, S. A. Song, A. L. Chuvilin, A. K. Gutakovskii, A. V. Latyshev, *Microscopy of Semiconductor Materials*, Springer Proc. Physics, Vol. **107**, 359–362 (2005).
28. M. Dionízio Moreira, R. H. Miwa, P. Venezuela, Phys. Rev. B, **70**, 115215 (2004).
29. C. Leroy, P. G. Rancoita, Rep. Prog. Phys., **70**, 493–625 (2007).
30. B. R. Gossik, J. Appl. Phys., **30**, 1214–1218 (1959).
31. L. Marqués, L. Pelaz, P. López, I. Santos, M. Aboy, Phys. Rev. B, **76**, 153201 (2007).
32. N. E. B. Cowern, G. Mannino, P. A. Stolk, F. Roozeboom, H. G. Huizing, J. G. van Berkum, F. Cristiano, A. Claverie, M. Jaraíz, Phys. Rev. Lett., **82**, 4460–4463 (1999).
33. J. Kim, F. Kirchhoff, J. W. Wilkins, F. S. Khan, Phys. Rev. Lett., **84**, 503–506 (2000).
34. A. Bongiorno, L. Colombo, F. Cargnoni, C. Gatti, M. Rosati, Europhys. Lett., **50**, 608–614 (2000).
35. G. D Watkins, J. W Corbett, Phys. Rev., **121**, 1001–1014 (1961).
36. A. K. Ramdas, M. G. Rao, Phys. Rev., **142**, 451–456 (1966).
37. H. J. Stein, Phys. Rev., **163**, 801–808 (1967).
38. L. C. Kimerling, H. M. DeAngelis, J. W. Diebold, Sol. St. Comm., **16**, 171–174 (1975).
39. Young-Hoon Lee, J. W. Corbett, Phys. Rev. B, **13**, 2653–2666 (1976).
40. B. L. Gregory, C. E. Barnes, in *Radiation Effects in Semiconductors*, ed. F. L. Vook, Plenum Press New York, 1968, p. 124.
41. C. A. Londos, Phys. Rev., B **53**, 6900–6903 (1996).
42. G. D. Watkins, K. L. Brower, Phys. Rev. Lett., **36**, 1329–1332 (1976).
43. L. W. Song, G. D. Watkins, Phys. Rev. B, **42**, 5759–5764 (1990).
44. M. T. Asom, J. L. Benton, L. C. Kimerling, Appl. Phys. Lett., **51**, 256–258 (1987).
45. G. Davies, Semicond. Sci. Techn., **4**, 327–330 (1989).
46. M. Draghici, L. Jdira, V. Iancu, V. Ioannou-Sougleridis, A. Nassiopoulou, M. L. Ciurea, Proc. IEEE CN 02TH8618, Int. Semicond. Conf. CAS 2002, **1**, 119–122 (2002).
47. M. L. Ciurea, V. Iancu, M. R. Mitroi, Solid State Electron., **51**, 1328–1337 (2007).
48. V. Ioannou-Sougleridis, A. G. Nassiopoulou, M. L. Ciurea, F. Bassani, F. Arnaud d'Avitaya, Mater. Sci. Eng. C, **15**, 45–47 (2001).
49. V. Ioannou-Sougleridis, V. Tsakiri, A. G. Nassiopoulou, F. Bassani, S. Menard, F. Arnaud d'Avitaya, Mater. Sci. Eng. B, **69–70**, 309–313 (2000).
50. D. A. Faux, J. R. Downes, E. P. O'Reilly, J. Appl. Phys., **82**, 3754–3762 (1997).

51. A. Benfilda, Proc. 1st Int. Workshop Semicond. Nanocryst. SEMINANO 2005, **1**, 123–126 (2005).
52. G. Bersuker, P. Zeitzoff, J. H. Sim, B. H. Lee, R. Choi, G. Brown, C. D. Young, Appl. Phys. Lett., **87**, 042905 (2005).
53. D. J. Meyer, N. A. Bohna, P. M. Lenahan, A. J. Lelis, Appl. Phys. Lett., **84**, 3406–3408 (2004).
54. M. L. Ciurea, M. Draghici, S. Lazanu, V. Iancu, A. Nassiopoulou, V. Ioannou, V. Tsakiri, Appl. Phys. Lett., **76**, 3067–3069 (2000).
55. M. Draghici, M. Miu, V. Iancu, A. Nassiopolou, I. Kleps, M. L. Ciurea, Phys. Stat. Sol. (a), **182**, 239–243 (2000).
56. V. Iancu, M. L. Ciurea, M. Draghici, J. Appl. Phys., **94**, 216–223 (2003).
57. M. L. Ciurea, I. Baltog, M. Lazar, V. Iancu, S. Lazanu, E. Pentia, Thin Solid Films, **325**, 271–277 (1998).
58. M. L. Ciurea, V. Iancu, V. S. Teodorescu, L. C. Nistor, M. G. Blanchin, J. Electrochem. Soc., **146**, 3516–3521 (1999).
59. S. Huang, S. Oda, Appl. Phys. Lett., **87**, 173107 (2005).
60. R. J. Walters, G. I. Bourianoff, H. A. Atwater, Nature Materials, **4**, 143–146 (2005).